

Optimization of structure and properties of WC-reinforced FeCoNiCr high-entropy alloy composite coating by laser melting

Yao Ju^{a,b,*}, Ievgen Konoplianchenko^b, Jiafei Pu^b, Zhengchuan Zhang^b, Qi Dong^b, Mykhailo Dumanchuk^b

^a Xinxiang Vocational and Technical College, Xinxiang, 453000, China

^b Sumy National Agrarian University, Sumy, 40021, Ukraine

ARTICLE INFO

Keywords:

Tungsten carbide
High-entropy alloys
Microhardness
Composite coatings
Impact resistance
Material applications

ABSTRACT

High entropy alloys have the potential to be used as coating materials in many fields due to their excellent mechanical properties, corrosion resistance and high-temperature stability. Based on the application requirements of high-entropy alloys, this study aims to explore how tungsten carbide can optimize the properties of high-entropy alloys. Through theoretical research and experimental validation, the effects of the organizational structure of high-entropy alloy coatings on their properties and the effects of tungsten carbide content on the properties of high-entropy alloy coatings were investigated. The micro hardness of the coatings is relatively high at low power laser melting, while it decreases with the increase of laser power. After laser melting of different materials, the average impact toughness of the studied materials exceeded 70 J/cm², and the average values of microhardness of the optimized coatings prepared at laser powers of 1400 W and 1600 W were more than 160 HV0.2. In addition, the properties of the high-entropy alloys were significantly improved when the content of tungsten carbide reached a certain percentage. The composite coatings have excellent wear resistance, corrosion resistance and thermal stability. Overall, the optimized tungsten carbide on high entropy alloys in this study has good performance, which is of great theoretical and practical significance for understanding the performance regulation and optimal design of high entropy alloy coatings.

1. Introduction

In the past few decades, high-entropy alloys (HEAs) have attracted much attention from scientists and engineers due to their unique properties and wide range of application prospects. HEAs are alloys formed by five or more principal elements in nearly equiatomic proportions, and they have excellent mechanical properties, corrosion resistance, and thermal stability [1–3]. However, despite the many advantages of high-entropy alloys, the hardness and wear resistance still need to be improved. In this context, researchers have started to explore the improvement of hardness and wear resistance of HEAs by adding hard particles, such as carbides, nitrides and borides. Among them, tungsten carbide (WC) is considered as the most promising reinforcing phase due to its extremely high hardness and stability. However, the research on combining WC with high-entropy alloys is still very limited, especially the preparation of WC-reinforced composite coatings of HEAs by laser melting and cladding techniques [4–6]. Laser cladding is a surface

modification technique that can form a coating with excellent properties on the surface of the substrate. This technique has the advantages of a small heat-affected zone, fast cooling speed, and strong bonding between the coating and the substrate. However, it is still a challenge to prepare WC-reinforced HEA composite coatings with uniform structure and excellent performance by laser cladding technology. In addition, although FeCoNiCr high-entropy alloy has been widely studied for its excellent mechanical properties and corrosion resistance, its application in laser melting cladding WC-reinforced composite coatings is still rarely reported [7–9]. Therefore, how to optimize the composition and process parameters of FeCoNiCr high-entropy alloys to obtain the best coating properties is also an important topic of current research. In summary, the structure and property optimization method of laser melting cladding WC-reinforced FeCoNiCr high-entropy alloy composite coatings will be explored through systematic experimental studies. It is hoped that this study will provide new theoretical and practical guidance for the preparation and application of HEA composite coatings.

* Corresponding author. Xinxiang Vocational and Technical College, Xinxiang, 453000, China.

E-mail address: jy13353736578@163.com (Y. Ju).

<https://doi.org/10.1016/j.rineng.2024.101985>

Received 8 November 2023; Received in revised form 5 February 2024; Accepted 4 March 2024

Available online 12 March 2024

2590-1230/© 2024 The Authors. Published by Elsevier B.V. This is an open access article under the CC BY-NC-ND license (<http://creativecommons.org/licenses/by-nc-nd/4.0/>).

In this study, an innovative methodology is introduced in the field of High-Entropy Alloys (HEAs), and WC (Tungsten carbide) reinforced FeCoNiCr high-entropy alloy composite coating is prepared by laser melting technology, which not only breaks through the traditional alloy design principles, but also is based on in-depth theoretical research and experimental verification. The microstructure and properties of the high entropy alloy were optimized by making full use of the high hardness and stability of WC. In addition, we have for the first time explicitly analyzed the effects of different laser powers and scanning speeds on the properties of WC/FeCoNiCr composite coatings, and further enhanced the microhardness, wear resistance and impact resistance of high-entropy alloy coatings by precisely regulating the WC content, which is the first in this field. The unique gradient composite and alternating multilayer composite design not only improves the overall performance of the composite coating, but also provides new possibilities for application under different working conditions. The research results show that the high entropy alloy coatings optimized by WC can significantly improve various properties, which provides important experimental basis and theoretical support for the future application of high entropy alloy in industry and other high performance fields, and opens up a new direction for the study of high entropy alloy materials.

The first part of this research is used to analyze the current status of structure and property optimization of high-entropy alloy composite coatings, which leads to the subsequent content. In the second part, the optimization of FeCoNiCr high-entropy alloy composite coatings based on tungsten carbide laser cladding is proposed, which is the focus of this study. In the third part, the optimized high-entropy alloy coating is experimented, tested and compared with other high-entropy alloys. The fourth part is to analyze the results obtained from the experiments and summarize the shortcomings in the study.

2. Related works

High entropy alloy (HEA), as a special alloy system formed by five or more principal elements in nearly equal molar ratios, breaks the traditional alloy design principle and successfully realizes the design of multi-element coexisting alloys. With further research, high-entropy alloys have superior strength, corrosion resistance, and oxidation resistance. However, due to the thermal stability of HEAs not being high, their application areas are subject to certain limitations. The WRW team utilized laser cladding to create (CoCrFeNi)₉₅Nb₅ high entropy alloy coatings. They investigated how laser energy density affects the structure, hardness, and corrosion resistance of the coatings. Optimal process parameters yielded coatings with excellent properties. The study found that higher energy density results in a lower concentration of Cr₂O₃ and other elements in the coatings' surface passivation layer, which compromises corrosion resistance. The relative content of Cr₂O₃ and other elements in the passivation film on the surface of the coating decreases with the increase of energy density, which leads to a decrease of corrosion resistance [10]. H C team used high-speed oxygen fuel to prepare single face centered cubic high entropy alloy coating, and the results indicated that the heat of cavitation can induce grain growth and achieve structural relaxation [11]. DM Y et al. tested the optimization of the coatings by preparing multifaceted high entropy alloy coatings and combining with the CODE and other software, and the results of experiments indicated that the optimized coatings have high-temperature thermal stability, can be held in a vacuum for 2 h, and the optimized coating has high-temperature thermal stability, which can be held in a vacuum at high temperature for 2 h and has long-term thermal stability [12]. Feng et al. for optimization of biomedical alloys and found that elemental segregation often exists in conventional casting or arc melting processes. It greatly reduces the mechanical properties of biomedical alloys. The HEA with a three-cycle minimum surface lattice was optimally prepared, and the experimental results showed that its Young's modulus was between 6.71–16.21 GPa, which was close to that of human trabecular bone. By customizing the shape and porosity of the

TPMS lattice, the possibility of this structure to meet the requirements of various bone implants, affirms the Bio-HEA in biomedical applications [13].

In addition, in the enhancement of the properties of HEAs, H Su's team investigated the distribution of grain boundary features of Al_{0.3}CoCrFeNi high-entropy alloy by 5% cold rolling followed by heat treatment at 1000 °C for 1–100 h. It was found that the microstructure of the alloy contains FCC and ordered BCC (B2) structures. After annealing for 100 h, the alloy has a low -ΣCSL fraction of 71.34% and the largest specific boundary clusters, concluding that the grain boundary features have been effectively optimized. The research process exemplifies that the precipitation of B2 influences the overall mechanism evolution and provides a new way to optimize the grain boundary features [14]. Sajadr's team study used a vacuum induction melting process to prepare FeCrCuMn₂Ni₂ high entropy alloy ingots and hot forged them at 650–750 °C. Then the samples were annealed between 600 and 1100 °C for 2 h. The microstructural characteristics and mechanical properties were characterized. The experimental results showed that the hot-forged samples exhibited higher compressive yield strength and hardness but lower compressive strain. When the temperature exceeded 1000 °C, dissolution of precipitates was observed. When the annealing temperature exceeded 800 °C, the compressive yield strength decreased, and the compressive strain increased [15]. Although the above studies have achieved some results, it is also evident from the literature that these composite high-entropy alloys may result in inhomogeneity of composite properties and do not fully utilize the advantages of high-entropy alloys and hard particles. In addition, there is less research on the preparation methods of HEA coatings. Optimization studies of the structure and properties of the coatings are still very limited, especially the study of composite coatings prepared by laser melting has not been reported [16].

In summary, there is an urgent need to conduct an in-depth study on the laser melting of WC-reinforced FeCoNiCr HEA composite coatings in order to give full play to its superior performance in terms of hardness, corrosion resistance, thermal stability, and abrasion resistance, and to realize the wide application of this new material in the industrial field. The study aims to fill the gaps in this area, explore the optimal composite ratio and preparation process through rational design and optimization of experiments, so as to achieve a full range of composite coatings to improve the performance.

3. Optimization study of HEA composite coatings

To explore the preparation and optimization study of HEAs composite coatings. To optimize the performance, hard particles of tungsten carbide and materials with excellent corrosion resistance were selected as the base materials. A high-order solid-state laser enhancement system is selected for the preparation, and the laser power and scanning speed are optimized. Various performance tests were conducted. Two multi-coating structures were designed, namely, gradient composite and alternating multilayer composite. The gradient composite method improves the compatibility of different layers through gradient distribution and reduces the coating cracks. The alternating multilayer composite approach explores the impact resistance performance requirements by combining the soft composite coating fusion with the harder composite coating arrangement and alternating fusion.

3.1. High entropy alloy composite coating preparation and performance test research

The design and study of HEAs are mainly based on entropy configuration mixing theory, an approach that seeks to increase the stability of the phase by maximizing the configuration entropy. In high entropy alloys, the Gibbs free energy is calculated as shown in Eq. (1).

$$G = H - TS \quad (1)$$

In Eq. (1), G is Gibbs free energy. H is enthalpy. S is entropy. T is the absolute temperature. The mixed entropy value is calculated as shown in Eq. (2).

$$\Delta S_{mix} = -R \sum_{i=1}^n (c_i \ln c_i) \quad (2)$$

In Eq. (2), n is the main elements of the alloy, c_i is the atomic percentage of the corresponding element in the corresponding alloy system, and R is the Boltzmann constant. The common preparation methods of HEAs are displayed in Fig. 1.

In Fig. 1, the preparation methods can be categorized into six types, among which, heat treatment method is the initial and commonly used method to prepare high entropy alloys. Multiple elements are first mixed together in a certain proportion, and then the alloy is made by high temperature heat treatment. Rapid solidification method is mainly used to prepare amorphous high entropy alloys. By melting the raw material of the alloy at a very high temperature and then cooling it at a very fast rate to prevent the formation of crystalline structure. Co-mingling and mechanical ball milling methods are mainly used in powder metallurgy, where multi-element mixed powders can be effectively used to form alloys by mechanical ball milling and hot pressing. Direct synthesis methods include autoclave reaction, chemical vapor deposition, and laser selective zone melting. Rolling deformation methods are used to achieve rapid preparation of high entropy alloys by accelerating the solid solution process through the use of rolling deformation techniques. Electrochemical methods include electric arc furnace melting method and electrolysis method, etc. These methods can regulate the precision of elements to further improve the properties of HEAs. To enhance the strength of HEAs, hard particles are usually chosen to be mixed and fused in HEAs to enhance their strength and hardness, and common fused hard particles are such as tungsten carbide, silicon carbide, titanium carbide and so on. Among them, although silicon carbide has high hardness and good wear resistance, it is brittle under impact or high pressure, and the preparation cost is high. Titanium carbide has high hardness and high-temperature resistance, but its oxidation resistance is weak, and the production process of titanium carbide may produce harmful substances. In contrast, tungsten carbide has the obvious advantage of preventing plastic deformation of the material to a certain extent. Secondly it has a high fracture toughness, which reduces crack extension and improves the reliability of the workpiece. This study

focused on optimizing the preparation of composite coatings for high entropy alloys (HEAs). The alloy coatings exhibit a high melting point and stable performance in extreme temperatures due to good thermal stability. They also demonstrate good corrosion resistance. The base material selected for the study was 316L stainless steel, known for its molybdenum content and excellent corrosion resistance. This makes it an ideal candidate for comparison with the FeCoNiCr high entropy alloy. This characteristic can make it an ideal choice for comparison with FeCoNiCr high-entropy alloy. The material selection and pretreatment process are shown in Fig. 2.

The substrate used in this study was commercially available FeCoNiCr isotropic alloy with dimensions of 100 mm (length) \times 100 mm (width) \times 10 mm (thickness). The particle size of this powder ranges from 45 μm to 150 μm , and the powder has sphericity and uniform composition. Spherical cast tungsten carbide hard particle powder was chosen for the study which is commercially available with a particle size of 45 μm to 65 μm and the alloy powder was preheated in a vacuum drying oven before conducting the experiments. The actual picture of powder is shown in Fig. 3.

The coating preparation as well as the optimization process is shown in Fig. 4.

Before the tungsten carbide enhancement experiments, the tungsten carbide powder and FeCoNiCr high-entropy alloy powder were mixed in a specific mass ratio of 1:1, and then placed in a general commercial roller mixer to ensure that the tungsten carbide powder and FeCoNiCr high-entropy alloy powder were fully mixed. For the preparation of the coating, a high-order solid-state laser enhancement system, specifically a TruDisk 6006 model with 6000 W disc laser produced by Trumpf Company in Germany, was utilized, including a laser, an automated robotic arm, and cooling equipment. Helium was selected as the powder feeding gas source with nitrogen as the protective gas, and the flow rate was 2.5 L/min. During the experiments, in order to avoid the contamination of the base surface affecting the quality of the laser cladding, a hand-held grinder was selected to polish the substrate. To reduce thermal stress between the coating and substrate, a preheating process is implemented. After preheating, the molten coating is promptly removed. Involving the optimization of laser power and scanning speed, other fixed parameters are spot diameter of 0.4 cm, focal length of 0.17 cm, lap rate of 50%, and the powder feeding rate is controlled at 13.9 g/min.

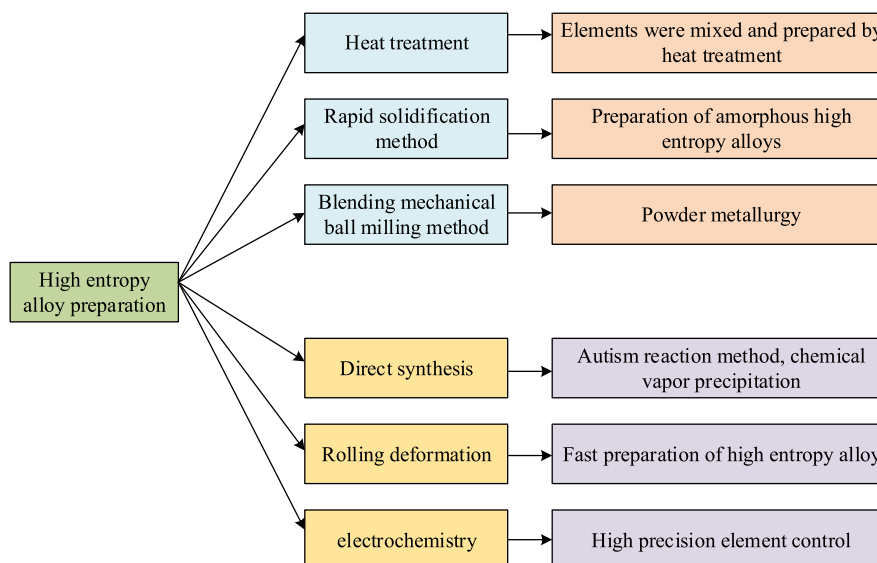


Fig. 1. High entropy alloy preparation method.

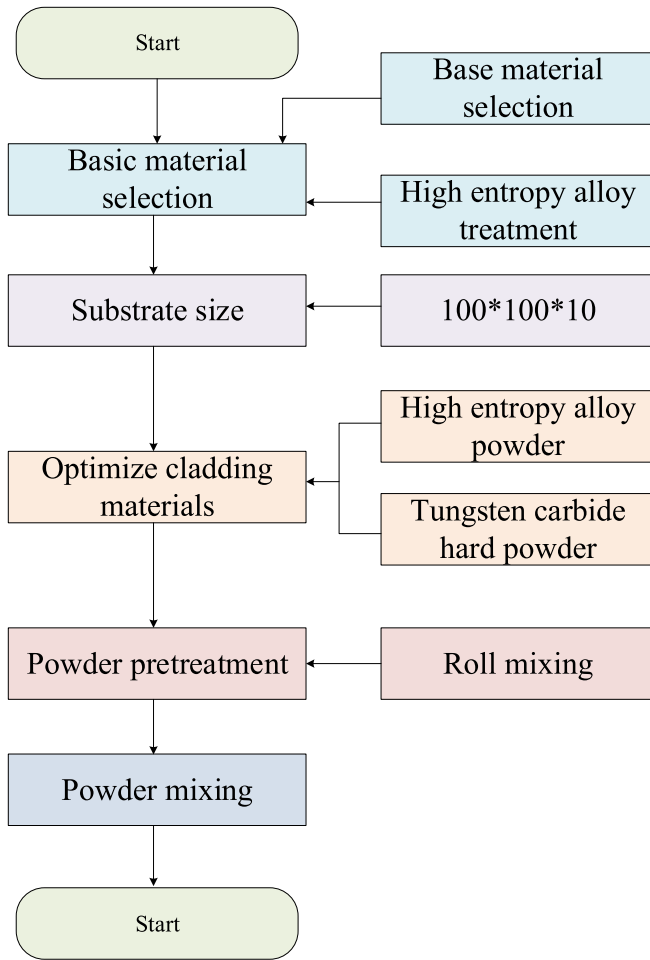


Fig. 2. Material selection and pretreatment process.

3.2. High entropy alloy coating process preparation

At present, due to the excessive choice of experimental parameters in the coating preparation of high entropy alloys, factors such as lap rate and spot diameter can play a key role in the coating quality. In the performance test, the high entropy alloy is tested from various aspects as shown in Fig. 5.

In Fig. 5, the flaw detection test employs ultrasonic testing (UT), a common non-destructive testing (NDT) technique for detecting internal and surface defects and cracks within the material. Metallographic analysis involves the observation of the alloy's microstructure using a

Leica Dmirm MW-550 optical microscope, which enables the identification of the grain structure and phase composition of the material., which can obtain information about the grain structure and phase structure of the material. Physical phase analysis is used to analyze the physical phase composition of high entropy alloys by X-ray diffraction, selected area electron diffraction, and other means. Microstructure analysis, on the other hand, is used to understand the microstructural characteristics of the alloy, such as grain size, dislocation density, and distribution of second-phase particles by observing the microstructure of the alloy [17–19]. In this case, the hardness increment after the addition of solid solvent in the coating can be expressed by Eq. (3).

$$H_s = 3^{\frac{2}{3}} \frac{G \epsilon_s^{3/2} C^{1/2}}{700} \quad (3)$$

In Eq. (3), G is the shear modulus, C is the atomic concentration of the solute, and ϵ_s is a constant that takes the value of 0.36. Microhardness testing, on the other hand, is an important measure of the hardness of high entropy alloys and their uniformity by indenting a small area and the ratio of the area of the indentation obtained to the load applied is called microhardness. The formula for the microhardness test is shown in Eq. (4).

$$H_v = \frac{F}{A} \quad (4)$$

In Eq. (4), H_v is the microhardness. F is the applied force. A is the indentation area. The wear resistance test is to evaluate the wear resistance of the HEA simulating the actual working environment for the wear test on the samples. In this case, the wear volume formula is shown in Eq. (5).

$$V = \pi \times S \times d \quad (5)$$

In Eq. (5), V is the wear volume, S is the cross sectional wear area and d is the wear diameter. The wear rate is calculated as shown in Eq. (6).

$$\zeta = \frac{V}{F \cdot L} \quad (6)$$

In Eq. (6), F is the loading load and L is the wear distance. The corrosion resistance test mainly detects the corrosion resistance of HEAs in a certain environment by immersion method and electrochemical method, and the corrosion rate can be calculated by Eq. (7).

$$C_R = (W_1 - W_2) / (A \times T) \quad (7)$$

In Eq. (7), W_1 is the mass before etching, W_2 is the mass after etching, A is the surface area of the sample, and T is the etching time. The most important parameters studied for coating preparation are laser power and scanning speed, and the laser energy density can be calculated by Eq. (8).

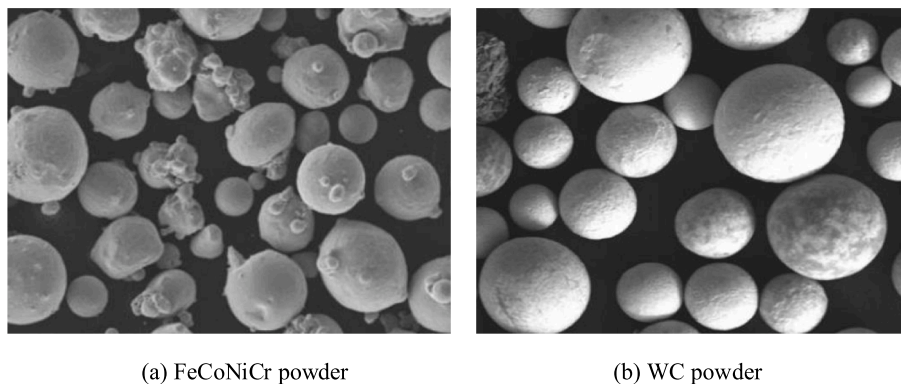


Fig. 3. Powder diagram.

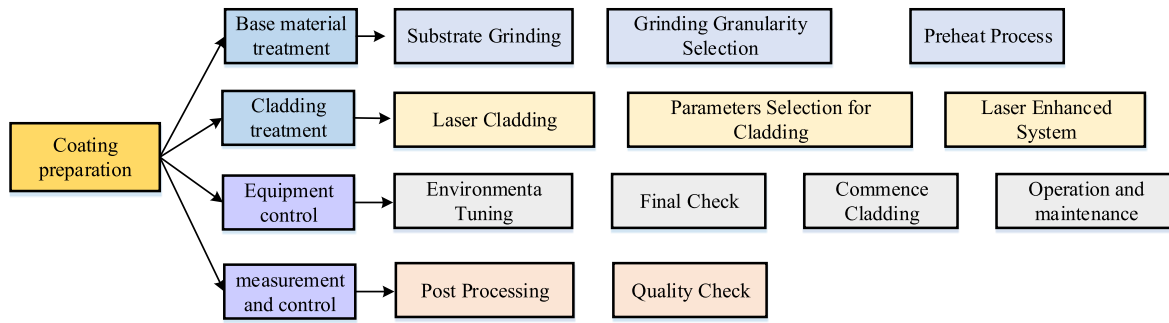


Fig. 4. Coating preparation and optimization.

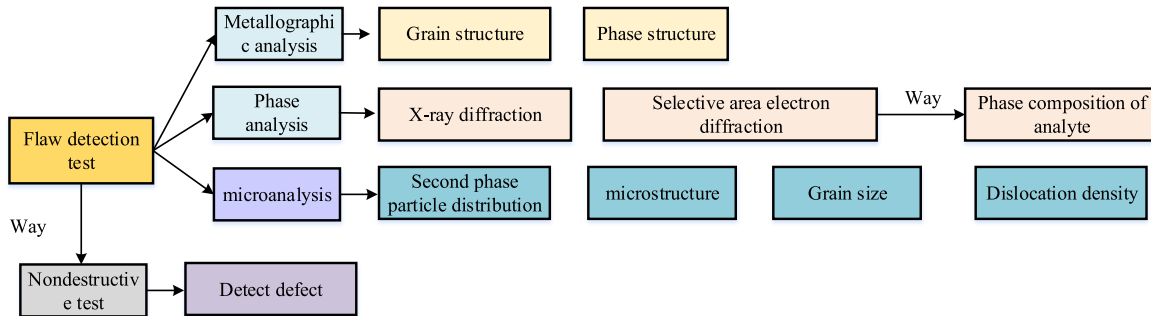


Fig. 5. Test method of flaw detection experiment.

$$P_b = \frac{4P}{\pi Dv} \tag{8}$$

In Eq. (8), P_b is the laser energy density, D is the spot diameter, v is the scanning speed, P is the laser power, and in the macroscopic morphology of the cladding layer, the dilution rate reflects the bonding of the coating to the material, which is calculated as shown in Eq. (9).

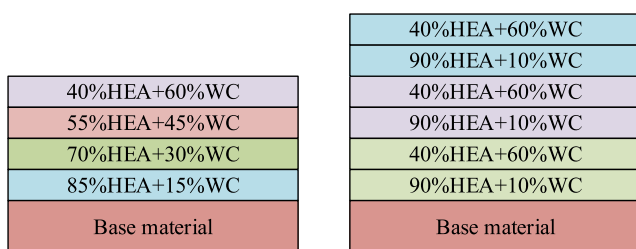
$$\eta = \frac{h}{H+h} \tag{9}$$

In Eq. (9), η is the dilution rate. H is the coating thickness. h is the melt pool depth. In the impact toughness calculation, as shown in Eq. (10).

$$a_k = \frac{A_k}{F} \tag{10}$$

In Eq. (10), A_k is the impact work and F is the cross-sectional area at the notch. Therefore, the design of the multi-coating structure of laser melted tungsten carbide reinforced high entropy alloy is shown in Fig. 6.

Fig. 6(a) depicts a gradient composite mode that increases material compatibility across different layers. This reduces cracking in the coating, suitable for various working conditions. The coating is approximately 4 mm thick, designed to prevent brittle cracks.



(a) Composite gradient coating (b) Composite alternate coating

Fig. 6. Optimization of multi-coating structure design for high entropy alloys.

Additionally, the surface layer is enhanced with tungsten carbide to boost corrosion and impact resistance. Fig. 6(b) shows an alternating multilayer composite mode, where softer and harder composite coatings are layered together. The softer coatings act as a transition between the layers, melted alternately to ensure the required impact resistance.

4. Analysis of the properties of tungsten carbide-optimized high-entropy alloys

Through theoretical research and experimental verification, to explore how tungsten carbide can optimize the properties of HEAs to provide new ideas and methods for the application of HEAs. The study analyzes the influence of the organizational structure of HEA coatings on their properties and investigates the influence of tungsten carbide content on the properties of high entropy alloy coatings. By changing the content of tungsten carbide, the effect on the hardness, wear resistance and other properties of HEA coatings is observed, and an attempt is made to find out the optimal content of tungsten carbide. Finally, the performance of multilayer composite coating structure is investigated [20,21]. By designing different composite coating structures, it will be explored how to further enhance the performance of high entropy alloy coatings through structural optimization [22,23].

4.1. Analysis of the influence of the organization and properties of HEAs coatings

All experimental steps in this study are strictly dependent on accurate and advanced experimental equipment. In order to ensure the accuracy of the experimental data, the main experimental equipment used in the experiment is listed in detail in Table 1.

Table 1 lists the experimental equipment used in this study and their uses. These include laser melting devices for preparing composite coatings, metallographic microscopy and scanning electron microscopy for microstructure analysis, X-ray diffractometer for phase analysis, microhardness tester for hardness testing, polishing machine and heat treatment furnace for sample pretreatment, wear testing machine and

Table 1
Experimental equipment and their purposes.

Equipment Name	Purpose
Laser Melting Apparatus	For laser melting of WC/FeCoNiCr composite coatings
Metallographic Microscope	To observe and analyze the microstructure of the alloy
X-Ray Diffractometer	For physical phase analysis of high entropy alloys
Scanning Electron Microscope	To analyze the microstructure and composition of the coating and substrate
Microhardness Tester	To measure the microhardness of the composite coatings
Grinding and Polishing Machine	For polishing treatment of the substrate surface
Heat Treatment Furnace	For preheating and heat treating the experimental samples
Wear Testing Machine	To test the wear resistance of the high entropy alloy coatings
Electrochemical Corrosion Tester	To test the corrosion resistance of the coatings

electrochemical corrosion tester for evaluating wear and corrosion resistance.

The study thoroughly analyzes the microstructure and properties of the HEA coating. It details the microstructure observations and examines the impact on the material's overall properties. The goal is to tailor the microstructure to enhance the performance of this new high-entropy alloy for applications. The microhardness of the single-pass fusion-coated layer is shown in Fig. 7.

Fig. 7(a) displays the line graph of the variation of microhardness of the cross-section of the cladding layer under different laser powers, with the increasing laser power, the microhardness decreases, and the microhardness decreases significantly when the laser power is more than 1800 W. At a laser power of 1000 W, the microhardness peaks at over 169 HV_{0.2}. Fig. 7(b) provides a line graph showing how interface microhardness varies with different scanning speeds. As scanning speed increases, microhardness significantly improves. At 2 mm/s, the microhardness initially drops and then rises, stabilizing near 159 HV_{0.2}. The highest microhardness, approximately 173 HV_{0.2}, is achieved at a scanning speed of 8 mm/s. In the physical phase analysis of the coatings, the XRD patterns of the HEA coatings prepared with different laser powers are shown in Fig. 8.

From the coating XRD plot in Fig. 8(a), it can be seen that the diffraction peak intensity ratio is more than 1 when the laser power is low, whereas it is less than 1 as the laser power continues to increase, allowing for the selection of an optimal orientation. It can be seen in the plot of peak intensities versus power in Fig. 8(b) that the intensities of both diffraction peaks (111 and 220) increase when the power is increased from 1200 W to 1400 W. However, the intensities of both diffraction peaks show a decreasing trend when the power is further increased to 1600 W. The intensity ratio of the diffraction peaks (111 and 220) is less than 1 when the power is increased to 1600 W. The

intensity ratio of the diffraction peaks is less than 1 when the power is increased. The value of (111) diffraction peak intensity/(220) diffraction peak intensity increases as the power increases from 1200 W to 1400 W, decreases slightly as the power continues to increase to 1600 W, and the ratio continues to decrease as the power is further increased to 2000 W. This indicates that with the increase in power, the change in the (220) direction is more significant, although the atomic arrangement is changing in both directions. The microhardness distribution of the coating cross-section at different laser powers is shown in Fig. 9.

From Fig. 9, the microhardness of the coatings prepared at laser powers of 1400 W and 1600 W is relatively high, with the average values of the respective microhardnesses being 162 HV_{0.2} and 167 HV_{0.2}. In the case of the HEAs, the possibility of lattice aberration is relatively small because of the small difference in the atomic radii of the four elements, namely, iron, cobalt, nickel, and chromium, which leads to the difficulty in significantly improving the microhardness of the coatings. And the microhardness of the coatings prepared when the laser power is lower than 1800 W, the performance is higher than the coatings prepared at 1800 W and 2000 W. Under low power conditions, where equal-sized grains are without preferred orientation, while the same-sized grains under high power conditions undergo the preferred orientation phenomenon, become irregular, and tend to the morphology of columnar crystals, and the degree of bonding between the grains gradually decreases, and the effect of microstrengthening decreases, and therefore the performance also decreases.

4.2. Study of tungsten carbide content on the properties of HEA coatings

Through the optimization experiments of the preparation process, it was determined that when the laser power was 1600 W and the scanning speed was 10 mm/s, the comprehensive performance of the prepared high-entropy alloy coating was excellent. When tungsten carbide particles are fused as reinforcing particles in HEAs, the corrosion resistance of the composite coatings can be effectively enhanced, etc. Therefore, the coating properties of tungsten carbide on HEAs with different contents is investigated.

Table 2 shows the EDS spot sweep results of different contents of tungsten carbide in composite coatings. And two samples are selected for comparison experiments, in sample A, with the increase of WC, the molar percentages of Cr, Fe, Co and Ni generally show a decreasing trend, while the molar percentages of W and C show an increasing trend, reflecting the increase of the relative weights of the elements W and C in the coating with the increase of WC content. In Sample B, also with the increase of WC content, the molar percentages of Cr, Fe, Co, and Ni largely decreased, especially Ni, which showed the most significant decrease from 0% WC to 60% WC content. At the same time, the molar percentages of W and C increased, notably for elemental W, from 0% WC to 60% WC content.

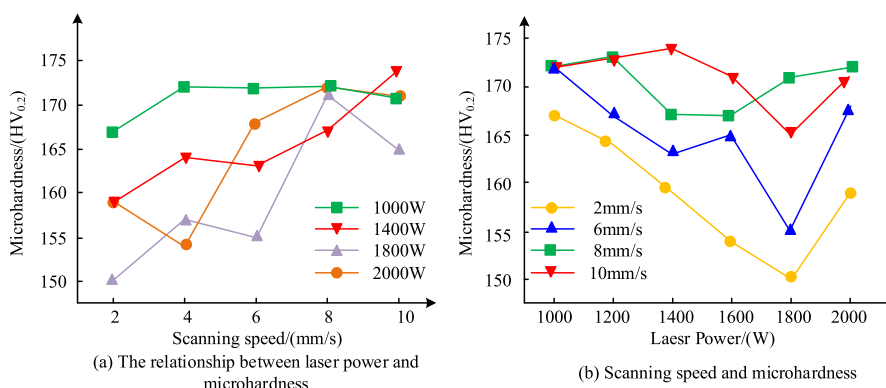


Fig. 7. Microhardness contrast curve.

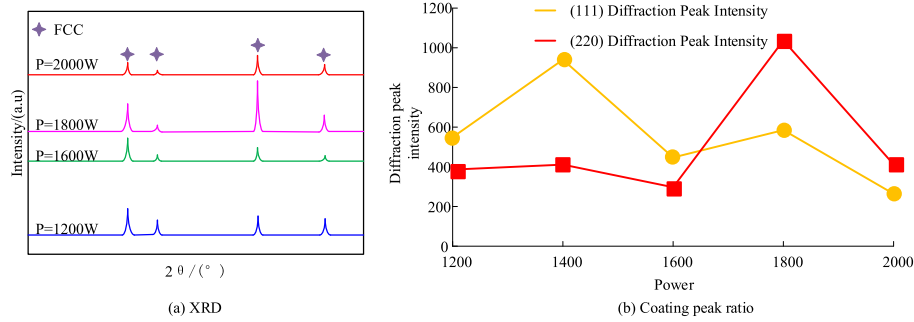


Fig. 8. Coating XRD pattern to peak ratio.

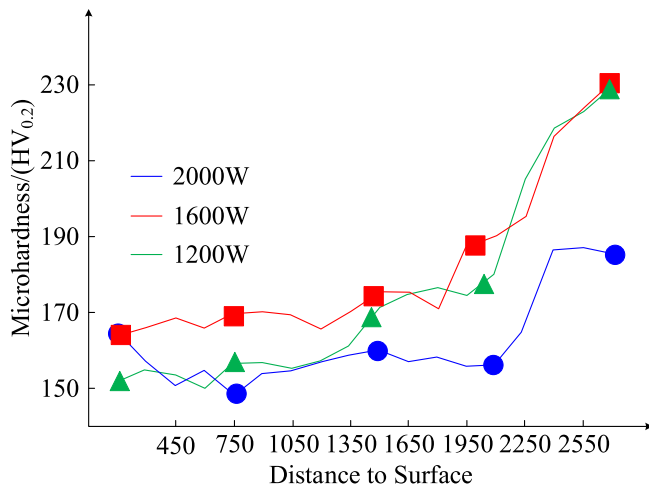


Fig. 9. Coating cross section microhardness distribution.

Table 2
Tungsten carbide fusion composite coating EDS dot sweep.

WC Content	Position	Cr	Fe	Co	Ni	W	C
0	A	25.62	30.31	23.1	22.05	/	/
0	B	27.95	29.01	21.94	21.93	/	/
0.1	A	21.31	38.95	16.58	17.99	1.99	4.78
0.1	B	35.98	25.39	12.8	9.82	8.65	9.32
0.2	A	23.61	29.88	20.81	21.5	1.56	4.83
0.2	B	42.59	20.98	13.66	10.82	3.41	10.24
0.3	A	23.83	28.94	21.69	20.88	1.69	4.88
0.3	B	39.65	21.8	14.87	11.79	4.38	8.93
0.4	A	20.98	33.94	19.72	20.7	2.39	4.38
0.4	B	41.78	21.69	12.79	9.43	7.89	9.92
0.5	A	19.26	36.42	18.98	20.84	3.31	4.75
0.5	B	32.67	23.83	12.6	9.45	12.93	10.24
0.6	A	19.43	30.54	20.87	22.25	3.52	6.58
0.6	B	31.96	19.39	14.47	11.49	13.33	13.36

4.3. Analytical study on the structural properties of multilayer composite coatings

The structural properties of a material are extremely important, which directly affect the life and effectiveness of the material in practical applications. Especially for multi-layer composite coatings, due to its structural characteristics, different layers may have different performance requirements and performance. Multi-layer composite coating refers to a coating with special properties made from two or more materials by fusion cladding, physical vapor deposition, and other processes. Such coatings offer significant surface performance advantages, such as excellent wear resistance, corrosion resistance or thermal

stability. However, the multilayer composite structure of the coating complicates the analysis of its properties. Various factors, such as different coating materials, thicknesses, mutual bonding properties and interface microstructures, can have impacts on the coating properties. Therefore, the performance of such coatings can be better understood and improved through in-depth structural performance analysis. The polarization curves in the corrosion resistance test of composite gradient coatings are shown in Fig. 10.

From Fig. 10, it can be found that the composites of gradient coating and single-layer 60% tungsten carbide coating have no obvious passivation area, and the self-corrosion voltage of single-layer 60% tungsten carbide special layer is higher than that of the gradient coating, and the current density is lower, and the corrosion resistance is better, and the tolerable arc radius of the single-layer tungsten carbide reinforced coating is significantly larger than that of the gradient coating, and the corrosion resistance is excellent. And in order to meet the research on the impact resistance of different parts, the impact resistance of the gradient coating is tested with the coefficient of friction, and the test results are shown in Fig. 11.

From Fig. 11, it can be found that after laser cladding of different materials, the average impact toughness of the studied optimized material reaches 74 J/cm², which is a good impact resistance advantage compared to other materials with close hardness. The impact toughness of 42 CrMoA cladding material is only 53.1 J/cm². Other hardness materials have even lower impact toughness, which will not be discussed.

5. Conclusion

High-entropy alloys are regarded as an ideal wear-resistant material

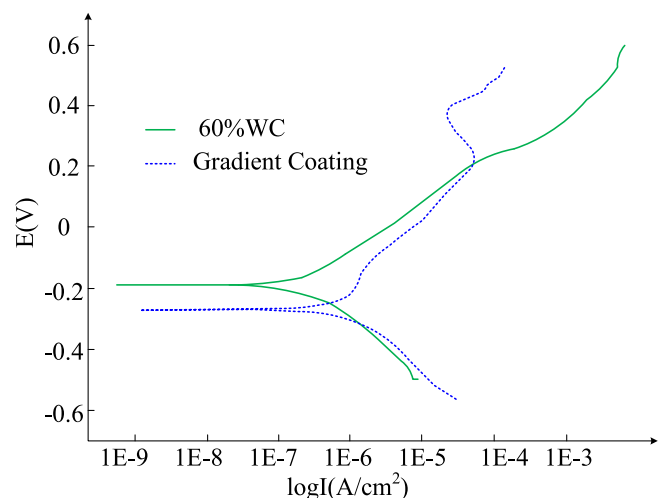


Fig. 10. Polarization curve.

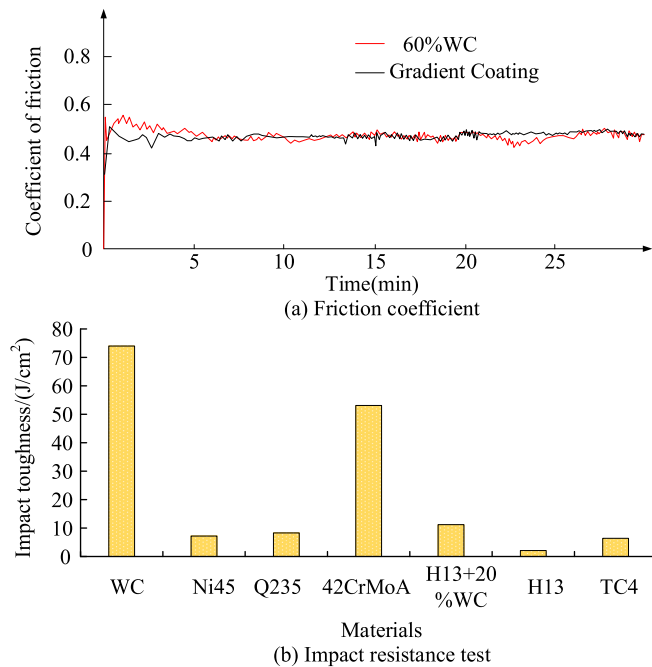


Fig. 11. Impact resistance test and friction coefficient test.

in aerospace and other fields due to their superior mechanical properties and thermal stability. However, its wear resistance still needs to be improved. The combination of the excellent properties of HEAs with the hardness advantage of WC particles may lead to performance optimization. It is investigated to optimize the properties of HEAs by adding tungsten carbide and to provide new ideas and methods for further applications of high-entropy alloys. When the study conducted an in-depth study of the organization of HEA coatings, the microhardness of the coatings was relatively high at low-power laser melting. The increase of laser power leads to the decrease of microhardness; the hardness reaches as high as 169 HV_{0.2} at 1000 W. The microhardness increases with the increase of scanning speed and reaches a maximum of 173 HV_{0.2} at 8 mm/s. Secondly, by changing the content of tungsten carbide, it is found that tungsten carbide can effectively increase the alloy hardness and wear-resistance, especially when the content of tungsten carbide reaches a certain proportion, the performance of high-entropy alloy is significantly enhancement. The composites with gradient coating and single layer of 60% tungsten carbide coating did not show obvious passivation areas, and the self-corrosion voltage of single layer of 60% tungsten carbide special layer exceeds the gradient coating, and the current density was lower and the corrosion resistance was better. Overall, the study initially revealed the mechanism of tungsten carbide's influence on the properties of HEAs, which is of great theoretical and practical significance for our understanding of the performance regulation and optimal design of high-entropy alloy coatings. However, studying still has some shortcomings. The study mainly focuses on a single tungsten carbide content and coating structure, for different contents and structures may have different performance effects, is a key direction for future research.

CRedit authorship contribution statement

Yao Ju: Writing – review & editing, Writing – original draft, Formal analysis. **Ievgen Konoplianchenko:** Formal analysis, Data curation. **Jiafei Pu:** Software. **Zhengchuan Zhang:** Visualization. **Qi Dong:** Formal analysis. **Mykhailo Dumanchuk:** Resources, Data curation.

Declaration of competing interest

The authors declare that they have no known competing financial interests or personal relationships that could have appeared to influence the work reported in this paper.

Data availability

Data will be made available on request.

References

- [1] W. Zhang, H. Xie, Z. Ma, H. Zhao, L. Ren, Graphene oxide-induced substantial strengthening of high-entropy alloy revealed by micropillar compression and molecular dynamics simulation, *Research* (1) (2023) 75–84.
- [2] T. Yu, H. Wang, K. Han, et al., Microstructure and wear behavior of AlCrTiNbMo high-entropy alloy coating prepared by electron beam cladding on Ti600 substrate, *Vacuum: Technology Applications & Ion Physics: The International Journal & Abstracting Service for Vacuum Science & Technology* 1 (199) (2022) 1–12.
- [3] K. Osintsev, S. Konovalov, V. Gromov, D. Zaguyliayev, Microstructure and phase composition of the Cr-Mn-Fe-Co-Ni high-entropy alloy obtained by Wire-Arc additive manufacturing, *Key Eng. Mater.* 910 (1) (2022) 748–753.
- [4] N.L.N. Broge, A.D. Bertelsen, F. Sndergaard-Pedersen, B. Bo, Facile solvothermal synthesis of Pt-Ir-Pd-Rh-Ru-Cu-Ni-Co high-entropy alloy nanoparticles, *Chem. Mater.* 35 (1) (2023) 144–153.
- [5] J. Liu, J. Hou, F. An, B. Qian, C.H. Liebscher, W. Lu, Characterization of compositionally complex hydrides in a metastable refractory high-entropy alloy, *Acta Metall. Sin.* 36 (7) (2023) 1173–1178.
- [6] H. Wang, Q.F. He, Y. Yang, High-entropy intermetallics: from alloy design to structural and functional properties, *Rare Met.* 41 (6) (2022) 1989–2001.
- [7] I. Hidayat, M.Z. Ali, A. Arshad, Machine learning-based intrusion detection system: an experimental comparison, *Journal of Computational and Cognitive Engineering* 2 (2) (2022) 88–97.
- [8] K.T. Atanassov, New topological operator over intuitionistic fuzzy sets, *Journal of Computational and Cognitive Engineering* 1 (3) (2022) 94–102.
- [9] A. Takeuchi, T. Wada, Os-Free Fe₁₂Ir₂₀Re₂₀Rh₂₀Ru₂₈ High-Entropy alloy with single HCP structure including Fe from late transition metals, *Mater. Trans.* 63 (1) (2022) 7–15.
- [10] W.R. Wang, Q. Wu, X.L. Zhang, X. Yang, L. Xie, D.Y. Li, Y.H. Xiang, Superior corrosion resistance-dependent laser energy density in (CoCrFeNi)₉₅Nb₅ high entropy alloy coating fabricated by laser cladding, *Minerals Metallurgy Materials* 28 (5) (2021) 888–897.
- [11] H. Cao, G. Hou, Z. Fu, Design of high-entropy alloy coating for cavitation erosion resistance by different energy-induced dynamic cyclic behaviors, *ACS Appl. Mater. Interfaces* 2 (15) (2023) 3651–3663.
- [12] D.M. Yu, C.Y. He, S.S. Zhao, H.X. Guo, G. Liu, X.H. Gao, A novel multilayer high temperature solar absorber coating based on high-entropy alloy NbMoTaW: optical properties, thermal stability and corrosion properties, *Journal of Materiomics* 7 (5) (2021) 895–903.
- [13] J. Feng, D. Wei, P. Zhang, Z. Yu, C. Liu, W. Lu, K. Wang, H. Yan, L. Zhang, L. Wang, Preparation of TiNbTaZrMo high-entropy alloy with tunable Young's modulus by selective laser melting, *J. Manuf. Process.* 85 (Jan) (2023) 160–165.
- [14] H. Su, Q. Tang, P. Dai, B2-precipitation induced optimization of grain boundary character distribution in an Al_{0.3}CoCrFeNi high-entropy alloy, *Journal of Alloys and Compounds: An Interdisciplinary Journal of Materials Science and Solid-state Chemistry and Physics* 918 (Pt.1) (2022) 1–10.
- [15] S.A. Sajadr, M.R. Toroghinejad, A. Rezaeian, Effect of annealing treatment on microstructural and mechanical properties of a hot-forged FeCrCuMn₂Ni₂ high-entropy alloy, *Materialia* 1 (26) (2022) 1–11.
- [16] J. Menghani, A. Vyas, S. More, C.P. Paul, S. Ingole, Preparation and characterization of laser clad AlFeCuCrCoNi high-entropy alloy (HEA) coating for improved corrosion performance, *Laser Eng.* 49 (1a3) (2021) 67–83.
- [17] N.X. Sheng, C.L. Qi, H.G. Yong, P.J. Li, Q.Z. Zhi, B. Lei, Ultrasonic flaw detection of discontinuous defects in magnesium alloy materials, *China Foundry* (4) (2019) 256–261.
- [18] D. Pranav, S. Sivaram, M. Nadarajan, A. Selokar, Behavior of heat treated aluminum alloy under hardness test, *Appl. Mech. Mater.* 903 (2021) 99–105.
- [19] G. Vimalan, Engineering stress-strain curves of inconel 600 alloy from high temperature tensile test, *Writers' J.: Journal of the Welding Research Institute* 3 (41) (2022) 18–28.
- [20] Q. Ma, B. Lu, Y. Zhang, Y. Wang, X. Yan, M. Liu, G. Zhao, Crack-free 60 wt% WC reinforced FeCoNiCr high-entropy alloy composite coating fabricated by laser cladding, *Mater. Lett.* 1 (324) (2022) 1–4.
- [21] X. Xian, Z.H. Zhong, L.J. Lin, Z.X. Zhu, C. Chen, Y.C. Wu, Tailoring strength and ductility of high-entropy CrMnFeCoNi alloy by adding Al, *Rare Met.* 3 (41) (2022) 1015–1021.
- [22] F. Shi, J. Zhao, M. Tabish, J. Wang, P. Liua, J. Chang, One-step hydrothermal synthesis of 2,5-PDCA-containing MgAl-LDHs three-layer composite coating with high corrosion resistance on AZ31, *J. Magnesium Alloys* 11 (7) (2023) 2541–2557.
- [23] T. Utkarsh, M. Somasundaram, B. Shalu Pargavi, U. NarendraKumar, A. Muthuchamy, A. Raja Annamalai, Investigating the impact of heat treatment on

the tribological behaviour of AZ80 magnesium alloy at high temperatures, Results in Engineering 21 (2024) 101661.